University of BRISTOL

Fiat 595 Abarth Convertible Roof Mechanism Design

Group Members: Darian Irani (en20703), Viral Shah (di20467), Andhika Nasution (ei20239)

Group 1a

Report date: 06/05/2022

Abstract

The assignment was to design a convertible roof mechanism for the Fiat 595 Abarth with an aim to put it in direct competition with the BMW Mini Cooper convertible. This report aimed to test the feasibility of a proof of concept, with the goal of mass production. Through the several stages of the project, concepts were rigorously assessed prioritising cost and safety and maintaining level performance. Combining technical analysis with thorough mechanical design, it was decided that this system would be developed and taken forward to the engineering team at Abarth.

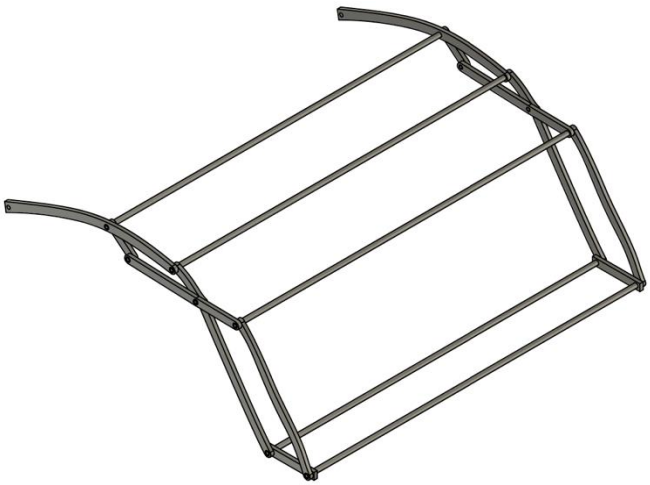

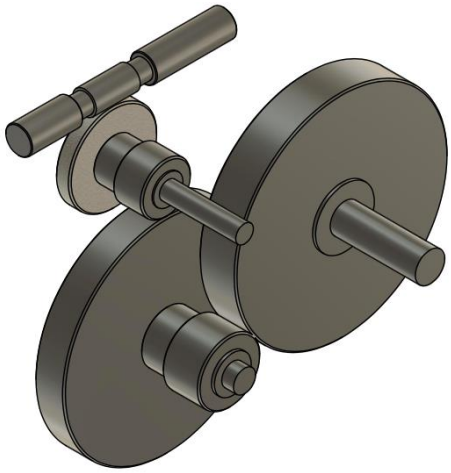

D1. Introduction

This project aims to produce a detailed design report for a convertible Fiat 595 Abarth that puts itself in direct competition with the BMW Mini Cooper convertible. Acting as the engineering team at Abarth, the following report presents a 'proof-of-concept design' for Fiat to take the idea forward into detailing and production based on the concept's viability for a convertible 595 Abarth. As a result, the report possesses a detailed consideration of the technical requirements, concept designs, motor & gearing analysis, gearbox layout, and design iterations.

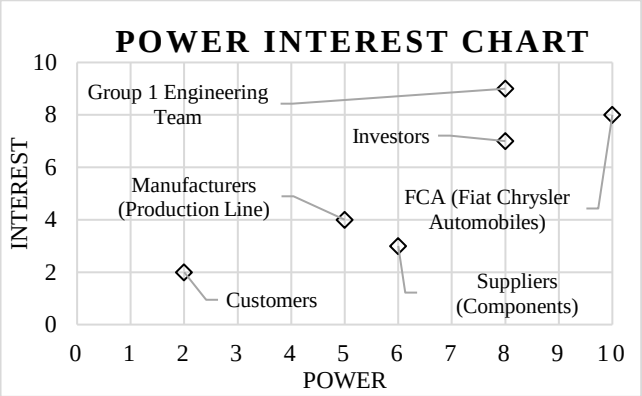

Figure 1: Power-Interest chart for stakeholders

Fig. 1 gives a numerical representation of stakeholder groups who have a direct interest and influence over the project – including manufacturing, performance, and overall quality control. Fig. A in the appendix provides a more detailed matrix about each stakeholder group.

Key priorities in the design were cost and safety. Cost was deemed a necessity due to the nature of this car within the market of affordable hatchbacks. Additionally, safety was prioritised with regards to customer satisfaction as well as investors reputation and likelihood to encourage further support. Two key assumptions made were: the engineering team has access to all components required to manufacture the mechanism – roof bracket, motor, gears, sensors & manufacturing methods; the engineering team has available budget in order to manufacture and conduct required research & development throughout the design process.

Fig. 2 displays an outline of the design process in the following report, showing a visual representation of how design decisions were made and how one output led to another. It shows the points in the report where the feasibility of concepts is questioned, indicating where iterations of the design were to be made.

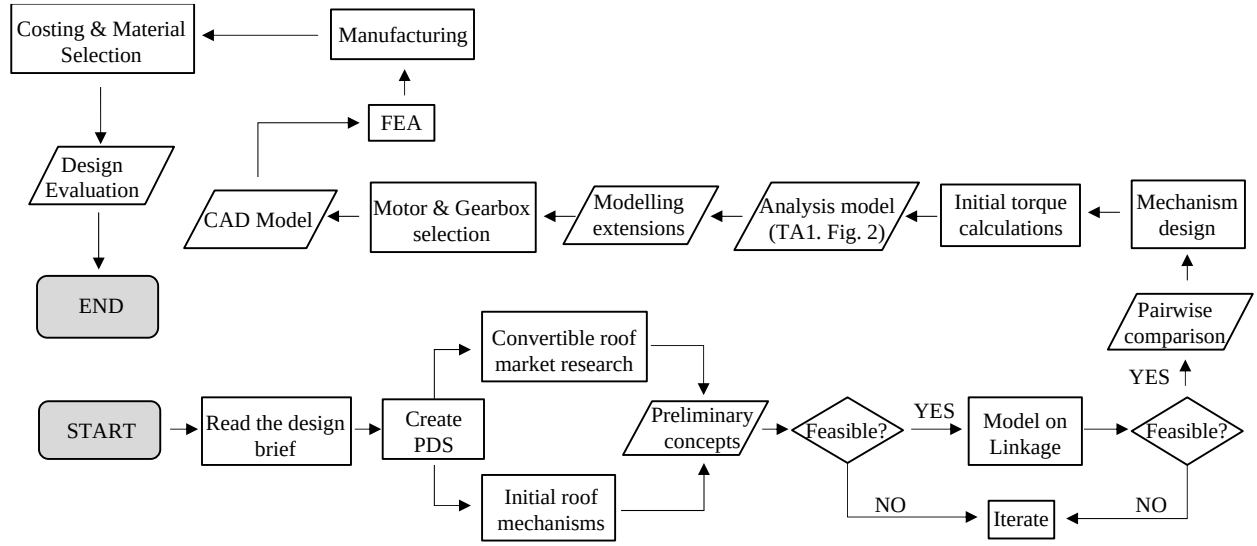

Figure 2: Flowchart depicting entirety of design process with ref. to Analysis Flowchart (TA1. Fig. 2)

D2. PDS

The PDS was generated using the design brief, market research and engineering intuition. The quantities in the target and limit columns were referenced from convertibles on the market and the MINI Cooper convertible. All the requirements are testable prior to the manufacturing of the car to supplement the design of the convertible Fiat. The requirements have a 5 to 1 priority ranking depending on their importance to the overall design of the roof where 5 is the utmost priority and 1 is the least priority. The highlighted requirements (1, 18) portray those not assessed in the PSS.

Table 1: Product Design Specification (PDS)

No.	Category	Requirement	Target	Limit	Test Method	Rank (5-1)
1	Safety	Should not interfere with headspace of passengers	150mm above headrest [1]	100mm above headrest	Run simulation on Linkage software	5
2	Safety	Roof should be able to withstand a certain weight	3000N [2]	2000N	Fusion stress analysis on mechanism.	5
3	Safety	Terminate folding process if obstacle is interfering with folding process	Obstacle detected 8mm away from car	Obstacle detected when in contact with car	Test sensor with Arduino	5
4	Safety	Terminate folding process if car is above certain speed	Process is terminated if speed > 20mph	Driver is alerted if speed > 20mph	Test sensor with Arduino	5
5	Safety	Terminate folding process if insufficient space above car	300mm above car	500mm above car	Test sensor with Arduino	5
6	Safety	Terminate folding process if headwind speed is too high	Process is terminated if speed > 20mph	Driver is alerted if speed > 20mph	Test sensor with Arduino	5
7	Performance	Components of roof should not be too complex	Total no. of members and joints: 25	Total no. of members and joints: 35	Run simulation on Linkage software	4
8	Performance	Folding mechanism should not use too much torque	Distance between deployed roof COM and pivot point: 600mm	Distance between deployed roof COM and pivot point: 800mm	Run simulation on Linkage software	3
9	Performance	Roof must operate perfectly in adverse weather conditions	Weatherproof casing for gearbox and joints	Weatherproof casing for joints	Market research for weatherproof casing	4
10	Performance	Folding process should be linear	Cycle time evenly split between motion phases	As balanced as possible	MATLAB inverse pendulum model	2
11	Performance	The roof must open and close within a given time	15 seconds [1]	20 seconds	Simulate model on MATLAB	5
12	Size	Roof must attach in given area	Attach in 80x80mm area [3]	Attach in 80x80mm area	Run simulation on Linkage software	3
13	Size	Roof must fold in given area	Fold in 670x280mm area, width 1204mm [3]	Fold within 670mm length, width 1204mm	Run simulation on Linkage software	3
14	Size	Total mass of roof mechanism should not exceed specified amount	25kg [4]	30kg	Fusion model	4
15	Size	Roof should be within a specified swept height	300mm above car [1]	500mm above car	Run simulation on Linkage software	3
16	Material	Mechanism should be recyclable	60% recyclable material	At least 30% recyclable material	Material selection	2
17	Material	Mechanism should be corrosion resistant	Non-oxidising material [5]	Corrosion resistant paint	Specs from Edupack software	3
18	Maintenance	Every component of roof must be detachable for servicing	Metal bracket and canvas replaceable (100% replaceable)	Canvas must be replaceable (50% replaceable)	Design decisions of the convertible roof	3
19	Maintenance	Components should be available by industrial standard	100% of components sourced via catalogues	50% sourced via catalogues	Market research on catalogues	3
20	Cost	Overall cost of roof mechanism	£500 [1]	£1000	Bill of materials	5
21	Aesthetics	Geometry should follow 595 Abarth roof structure	Follow curves of base model 595	Ensure no sharp turns in geometry	CAD model	2

D3. Concept generation

5 concepts were first sketched on paper as an initial prerequisite. Lego was then used as a basic reference, which was then translated into 3 concepts simulated in Linkage software as seen in Figs. 3, 4 and 5. This was an iterative process of using folding techniques along with Gruebler's Equation [18] (ensuring the number of members and joints coincided with degrees of freedom) and changing the geometry of members until they were fully extended and folded within the required dimensions. To gain a more accurate perspective of scale, an image portraying car dimension was overlayed onto the concepts (as seen in Figs. 3 to 6). Additionally, the test for cycle duration at this stage was simply a relative comparison between all the systems, with input rpm being an arbitrary constant common among the concepts.

D3.1. Concept 1

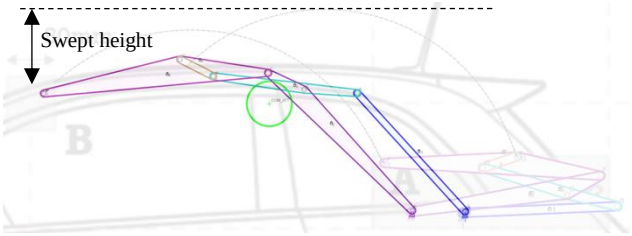

Figure 3: Concept 1

Looking at concept one (see Fig. 3), the applied mechanism was a derivative of the scissor mechanism. This is a low complexity, 5-bar design. Prioritising cost and performance, the simplicity of this design could reduce manufacturing costs and potentially increase reliability as fewer components are interacting with each other. This mechanism also does not interfere with the headspace of the passengers (PDS Requirement 1) which was tested on Linkage. Simulating opening the mechanism, the motion leaves an approximate space of 150mm between the roof and the user. The way concept 1 is designed, the swept height was minimised with a measured value of 253mm (Requirement 15). Reducing this reduces the overall surface area in contact with the air when opening, which can allow for the roof to be opened at greater velocities as the overall drag is reduced, in turn promoting safety.

D3.2. Concept 2

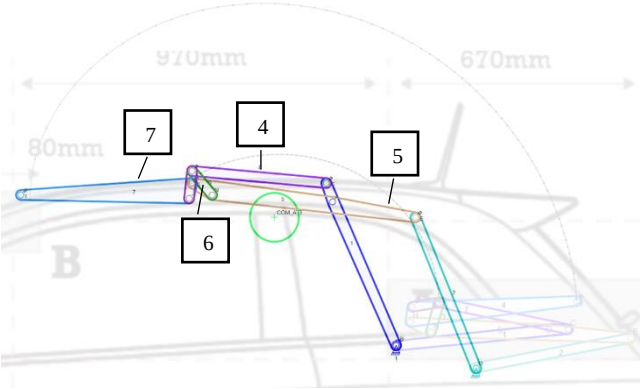

Figure 4: Concept 2

Concept two uses a 7-bar system, utilising a scissor mechanism with a front section that retracts backwards as it opens. This happens through the triangle of linkages connecting members 4, 5 and 7 as seen in Fig. 4, providing a creative way to collapse the roof. However, looking at the aforementioned triangle, there would be a high value of torque running through link 6, as the centre of mass is too far away from the pivot. Due to the way link 7 retracts, the swept height is much greater than the other concepts with a value of approximately 700mm. Having a large swept height would result in greater drag when opening the roof whilst the car is moving, therefore, stringent stress analysis testing must be implemented to ensure the safety of the passengers.

D3.3. Concept 3

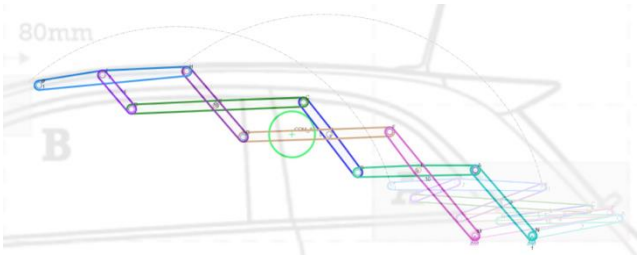

Figure 5: Concept 3

Finally, concept three is another form of a scissor mechanism, however, this time being a 10-bar system. This utilizes the most linkages out of all concepts, which could lead to a higher manufacturing cost and added complexities in maintenance. The fact that this is a common design throughout all linkage systems proves that it is a somewhat reliable concept, however, in this implementation having many links causes the length scaling and geometry to interfere with the back seats when fully extended. This poses a potential safety hazard. The swept height for this concept is the best of the three at 140mm, again allowing the operation of the roof to be more streamlined under higher wind speeds.

D3.4. Concept Selection Criteria

To determine the most suitable concept to take forward, a Pairwise comparison matrix found in Table 3 was used to compare the three concepts against weighted selection criteria. The calculated weightings shown in Appendix Table A uses important requirements from the PDS in Table 1. Each criterion, shown in Table 2, use different metrics to measure how they differ from each of the 3 concepts.

D3.5. Selected Concept

Table 3 displays a numerical representation of how each concept scored against the 7 criteria and their respective metrics. A ranking of ‘5’ being the best and ‘1’ being the worst, as a result, concept 1 scored the

highest overall percentage. This is reflected by concept 1 for its minimal components and joints, resulting in a low mass system with realistic costs and torque requirements.

Table 2: Concept selection criteria metrics

Complexity - proportional to the number of joints the concept requires.	**Safety** - measured by considering how much space the roof takes up inside the car during its folding process.
Max Height - the tallest point of the roof during the folding process.	**Cost** - proportional to the sum of members and joints the concept requires (assuming each member costs the same).
Mass - proportional to the number of members the concept requires.	
Torque - distance between the concepts' COM and its pivot point.	**Stowed Away Size** - the dimensions of the roof when folded.

Although it ranks second for its maximum swept height, it is only 80mm higher than concept 3 which ranked first. Finally, concept 1 also ranked first for its safety as it interferes the least with the backseat passengers' headspace, which ultimately results in the best stowed away size. Therefore, the consensus was to go ahead with concept 1 as the selected concept since it scored the highest in the weighted matrix and is most in line with the requirements stated in the PDS.

Table 3: Pairwise comparison matrix

	Criteria	Complexity	Max height	Mass	Torque	Safety	Cost	Stowed away size		
	Weights	0.130	0.193	0.028	0.021	0.363	0.245	0.021		
Options		1	2	3	4	5	6	7	Total	%
Concept 1	1	4	2	3	2	4	4	3	3.524	52.3
Concept 2	2	2	3	2	1	2	2	2	2.172	32.2
Concept 3	3	1	1	1	3	1	1	1	1.042	15.5

D4. Mechanism Design

Note: Motor, gear ratio and damping coefficient selection was carried out using the retraction model, as this is what had the longer cycle time when compared to deployment. The holding ratio was the gear ratio needed to keep the mechanism in a deployed (unattached) position, as retracting from here needs the highest torque.

D4.1. Geometry Iteration

As an iteration for the design of the members, the geometry was altered so that the roof mechanism would be more realistic. The previous design consisted of straight members as seen in Fig. 6, but the problem arises when the roof material lays over the system. The top of the Abarth 595 has a smooth gradient throughout so replacing it with clear-cut straight edges will negatively affect the aesthetics of the vehicle. The roof geometry was revised so that the outer members in contact with the roof provided a smooth gradient seen in Fig. 7, thus, further satisfying Requirement 21 in the PDS.

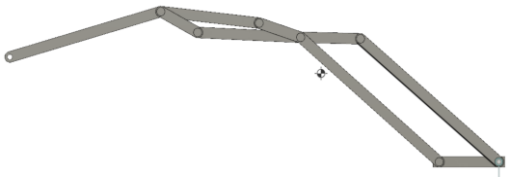

Figure 6: Initial member geometry

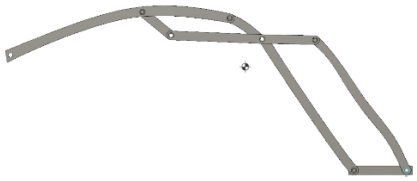

Figure 7: Concept 1

D4.2. Material Selection

$$M_{Stiff\ ,Mass} = \rho/\sqrt{E} \quad (1)$$

$$M_{stiff\ ,Cost} = C_m\rho/\sqrt{E} \quad (2)$$

$$M_{Strengt\ h,Mass} = \rho/(\sigma_y)^{\frac{2}{3}} \quad (3)$$

$$M_{Strengt\ h,Cost} = C_m\rho/(\sigma_y)^{\frac{2}{3}} \quad (4)$$

Where ρ is density, E is Young's modulus, C_m is the cost per unit mass and σ_y is the yield stress.

The material selected for the roof mechanism was found by applying conflicting objective equations and determining a corresponding material index. Minimising mass and cost were the primary objectives which further align with Requirements 14 and 20, respectively, in the PDS. A stiffness and strength constraint were applied, modelled for a beam of length L and force F to represent a single member in the system. In both stiffness and strength limited design, the free variable was the material (density) and the area of the beam.

The loading conditions modelled for both design scenarios were a simply supported universally distributed load which was concluded to be the most accurate depiction for a convertible car roof. After eliminating the free variable, the material indices for stiffness and strength limited design can be seen in (1), (2), (3) & (4).

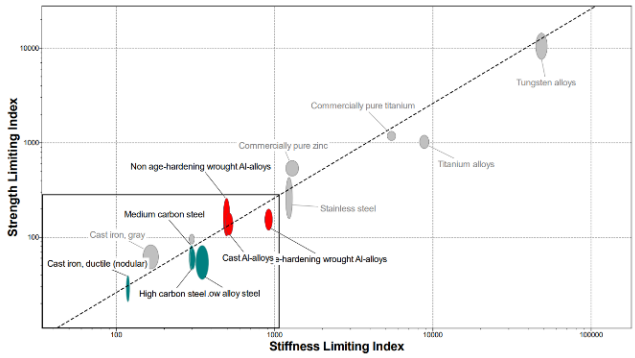

Figure 8: Minimise mass with stiffness and strength limited constraint

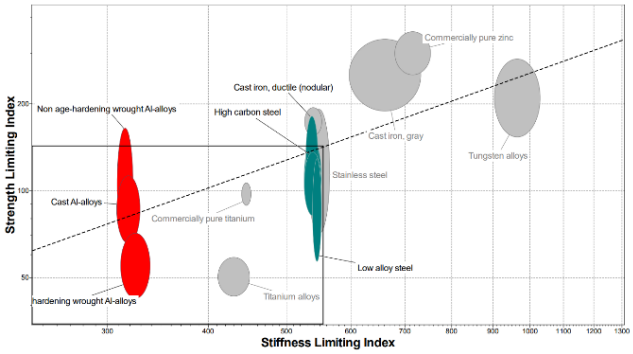

Figure 9: Minimise cost with stiffness and strength limited constraint

On Granta Edupack [7], 2 graphs were plotted of the material indices $M_{Stiff,Mass}$ against $M_{Strength,Mass}$, and $M_{stiff,Cost}$ against $M_{Strength,Cost}$ seen in Figs. 8 and 9. A line representing the indices' coupling constant, was plotted on each graph alongside a box selection with the limits of required strength and stiffness. Edupack conveniently narrows down the material options so that only materials within both box selections remain.

For a robust method to compare the remaining materials, a weighted matrix with criteria: density, cost per unit mass, Young's modulus, yield strength, tensile strength and compressive strength was used, shown in Table B in the appendix. Each criterion was assigned a weighted value, dependent on its importance, with values for each criterion completely sourced through the material data sheets on Granta Edupack. Each material was then given a score depending on how well it performed in each criterion with the final material determined to be low alloy steel.

D4.3. FEA Stress Analysis

As a final consideration for the definitive design, an initial CAD model was developed in Fusion 360 with an assumed bar thickness of 12mm. Applying a static stress simulation when the system is deployed, the outputs can be analysed such that a compelling value for thickness can be determined. Minimizing thickness decreases the overall mass of the system and in doing so, follows Requirement 14 in the PDS. The simulation was also tested against Requirement 2.

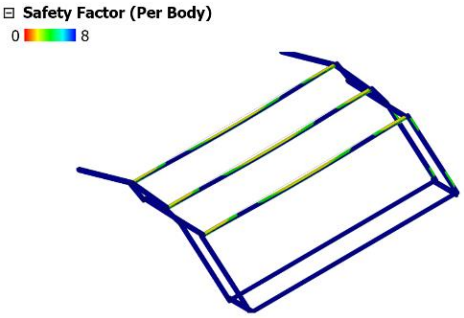

Figure 10: Safety factor stress analysis results when deployed.

For the initial loading case, a static stress simulation was conducted. The effects of gravity, universally distributed loads and wind loading were applied normally across each face of the top beams with a magnitude of 2000N. The study material chosen was low alloy steel which was determined in the D4.2.

When analysing the simulation results, the safety factor, Von-Mises stress and displacement were the outputs taken into consideration. From the safety factor output graphs, it is clear that areas with the lowest safety factors are situated on the lateral beams which are connecting the two mechanisms. The lowest minimum safety factor was 1.041 as seen in Fig. 10, which is not within a particularly safe region, but sufficient for the limits of Requirement 2. Nevertheless, the safety factor across the other beams can be seen in blue, meaning that the value can lie from 6 to 15 which is within a comfortable safety range. An argument can be made that it is unlikely a load of 2000N would be experienced, however as a safety concern, when the car is travelling at a high velocity alongside harsh weather conditions, the roof can be exposed to excessively high loads. A solution to improve the safety factor in the lateral beams was to increase their diameter, whilst maintaining the same thickness for the remaining beams. Extending this, the results from the Von Mises stress and displacement analysis support the lack of strength in the lateral beams as the greatest deflection and stress

concentrations occur in the middle of the members. Changing the diameter of the lateral beams to 15mm and repeating the static stress simulation when the roof is closed gives a minimum safety factor of 1.516 which now satisfies Requirement 2 in the PDS as the minimum load the roof can now withstand is 3032N.

D4.4. Fixings & Joints

The material selection process in D4.2 influenced the decision of choosing Alloy Steel plate 4140 material for the metal bracket of the convertible roof. Table 10 contains a full bill of materials showing all parts needed for the required fixings. The first type of fixing is a bush fixing at each of the 14 joints, which attach the ends of each member. The bush prevents friction between the joints and allows the joints to slide without wear in a rotary-like movement. This fixing uses a clearance fit at each joint where the bar is slightly slimmer than the rod holes. Additionally, a 1mm chamfer is machined into each member to aid assembly. This type of fit uses an h6H7 tolerance that is chosen to allow a hinge-like movement, which is important for the opening and closing of the convertible roof. Lateral movement in the joints and their members could lead to unwanted torsional stresses caused by wind forces or centrifugal acceleration. Therefore, two bearings are placed on each horizontal member to account for lateral displacement, using interference fits with p6H7 tolerances. The chosen bearing has a bore diameter of 15mm and the p6H7 tolerance leads to a 15.015-15.024mm range. The tolerancing and upper/lower bounds for diameter use Tables C and D in the appendix. The mechanism should work perfectly in adverse weather conditions as per PDS requirement 9; therefore, a waterproof covering is used to prevent rain from rusting the joints and dust from entering the joints' cavity.

D5. Damper Design

As outlined in TA2.3. damping was a feature, physically considered in the design to keep the utmost accuracy.

D5.1. Linear Damper

Firstly, a linear damper was added to the mechanism. Fig. 11 [8] show a design that inspired the final design used in this project, which is highlighted in Fig. 12. The Associated Spring Raymond [9] catalogue was used, and it was identified that using this type of configuration limited the cylinder length to 300mm. From this filtered selection, the 275.08mm damper was chosen as this offered the highest damping coefficient. Between the mechanism pivot and damper pivot, a connecting rod was used with radius equivalent to the stroke length, 101.6mm. The first and third lines show the points at which the damper is fully extended, with the second line showing the point of greatest compression. The dimensions on Fig. 12 differ to those stated previously as a different scale was used. The arc represents the path followed by the connecting joint, equivalent to part '402' from Fig. 11 and 'pivot a' represents 'part 266' on this same figure, which allows the damper to rotate and compress/extend through this motion.

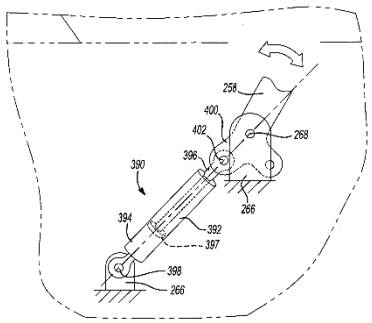

Figure 11: Exert from Patent US7275783B2 showing how the damper connects and extends as the mechanism moves.

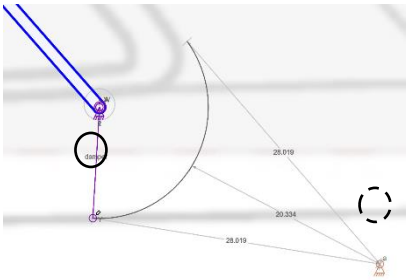

Figure 12: damper design in linkage

D5.2. Rotational Damper

Secondly, a rotational damper was considered, being fixed onto the initial layshaft in series with the motor. This would avoid using any connecting rods and directly apply torque to the input of the mechanism. In comparison this was a much simpler design, with the gearbox being joined in between via a pinion.

D5.3. Final Design

Whilst TA2.3. explains how the results from the linear damper were inferior to those from the rotational damper, the design also played a part in choosing against it. The main reasons were the scale and how much space the configuration took up. Also, being a dynamic system with moving parts, there extra joints and fixings which decrease the overall safety of this feature and is more prone to required maintenance and hence lifetime cost, which were two priorities of this project. On the other hand, rotational dampers have no moving parts

and are permanently sealed, making them more durable and requiring little maintenance [10]. The high viscosity fluid inside the damper also absorbs external shock and vibration, therefore increasing its safety.

D6. Motor, Gear Ratio & Damping Coefficient Selection

D6.1. Initial Motor Analysis

Through the design brief, it was required that DC motors from the Bosch catalogue, [11] without transmission were to be used, powered by the car battery at 12V. The motors chosen to carry out analysis were the APM and NSA-I motors. These were chosen because they featured clockwise and anti-clockwise rotation – a trait that prevents the need to implement a reverse gear train in the gearbox, in turn saving on mass and cost. The initial model also assumed a system mass of 20kg, which was then accurately calculated in D4.2. found to be 23.5kg and included in 6.2. Table 4 shows holding ratios for all motors.

Table 4: Holding ratios for all candidate motors.

Motor	Holding Ratio	Motor	Holding Ratio	Motor	Holding Ratio	Motor	Holding Ratio
APM	601.4	NSA-I 1	265.7	NSA-I 2	238	NSA-I 3	165.6

Initially, with only the motor and gravity acting on the system, the four motors were tested with gear ratios 1% above their holding ratio. Depicted in Figs. 13 and 14 and are their retraction times and efficiency, showing that the APM motor was the closest to the required cycle time, as well as having the highest efficiency. On the other hand, it was noted that the gear ratio was also the highest at well over double all the NSA-I motors. As extensions were added to the model to increase resistive torques to the mechanism, the gear ratio was predicted to increase due to this motor's very low stall torque. This was an important factor when considering gearbox design as higher gear ratios lead to larger, heavier, and more expensive gearboxes, and with cost being a design priority this resulted in the APM motor being discarded. The NSA-I 2 motor was also set aside, but not discarded, due to its very high running speeds and high nominal power as per the Bosch Catalogue. This left NSA-I 1 and 3, the latter having the second highest efficiency. Therefore, the NSA-3 motor was chosen at this stage, even though it had a very quick cycle time.

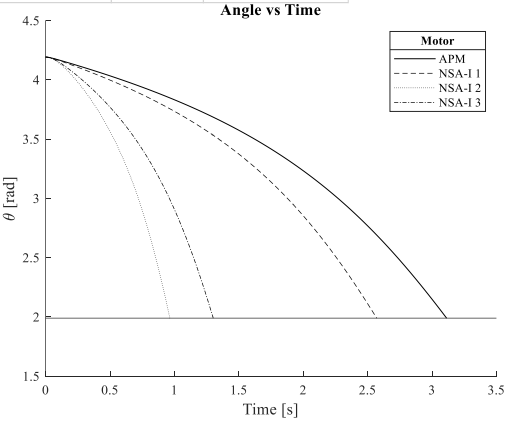

Figure 13: Cycle time for all motors

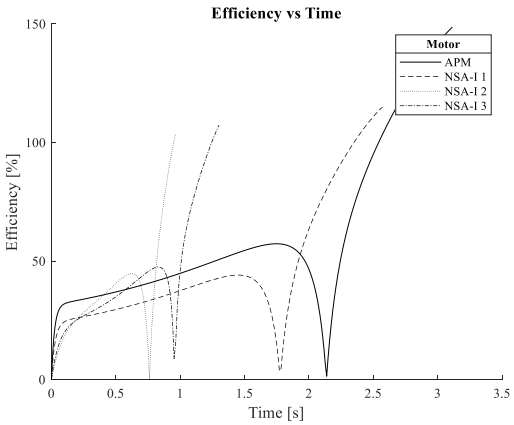

Figure 14: Efficiency for all motors

D6.2. Final Motor Analysis

In this section the complete model, inclusive of 20mph oncoming wind, was considered. The gear ratio and damping coefficient were selected as a combination and as such, iterated together. The design priorities, as per Requirements 11 and 10 in the PDS, were to obtain cycle time between 15 and 20 seconds, whilst aspiring to have motion as linear as possible. To achieve this, it was found through comparison of high and low, that higher damping coefficients favoured this motion. This is because higher speeds are affected more by damping, with lower speeds remaining similarly low across different coefficients. Due to this, a higher stall torque would be favoured as lower gear ratios would achieve similar performance to motors with lower stall torque and higher gear ratios. At first, a damping coefficient of 1000Nmsrad^{-1} was used to compare properties of the three motors at a gear ratio of 50% above the holding ratio. The

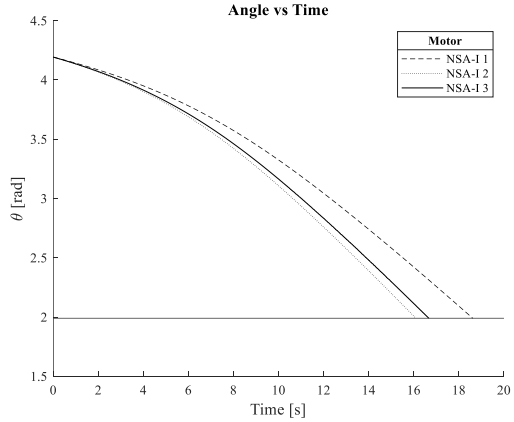

Figure 15: Cycle time for all motors

resulting cycle times are presented in Fig. 15 for all motors. Power usage and efficiency were not priorities in motor selection; hence their outputs were not utilised – they can be seen in Figs. D and E in the Appendix.

D6.3. Final Value Selection

A manual process of checking combinations of gear ratio, damping coefficient for different motors took place. The aim of this was to fulfil Requirement 10, hence many iterations were considered. An exert of the full process being is displayed in Table 5, showing initial combinations that did not achieve linearity and final combinations that did. The rows highlighted are presented on Fig. 16 clearly showing that a low gear ratio and damping coefficient achieve a motion with a very steep gradient. The remaining curves are all linear motions for each respective motor, and it can be observed that, from left to right, the lines become slightly more linear. When referring to Fig. 16, it is evident that a higher damping coefficient favours a more linear motion – however this means higher gear ratios are required. Adhering to design priorities, the lowest gear ratio was preferential. The NSA-I 3 motor accommodated this preference as it was the most powerful motor, and as it was the lowest gear ratio to highest damping coefficient combination (see Table 5), these were the variables chosen. Also as seen in the final column, the range of 420-450 offered linear motions whilst still being under 20 seconds, hence this was the gear ratio range used in the gearbox design. The final characteristics are presented in Table 6 and Fig. 17 below, which were found using a gear ratio of 421.45 – this exact gear ratio and how it was calculated is outlined in D8.2.

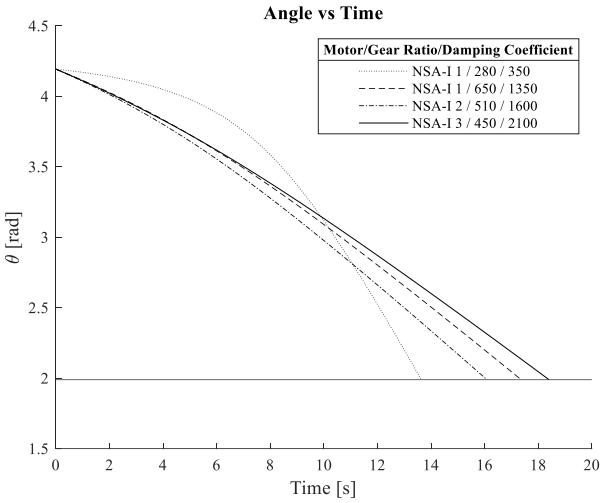

Figure 16: Cycle time for all motors

Table 5: Exert from thorough selection process, showing linear and non-linear combinations

Gear Ratio	Time [s]	Energy [J]	Efficiency [%]	Power [W]	Linear?	Gear Ratio	Time [s]	Energy [J]	Efficiency [%]	Power [W]	Linear?
NSA-I 1 / c = 350Nms/rad						**NSA-I 1 / c = 1350Nms/rad**					
280	13.6	202.4	10.3	26.9	N	580	18.9	381.7	14.9	24	N
350	9.7	222.7	18.3	29.8	N	610	18.1	396.6	16.7	25.5	Y
420	8.7	233.1	24.5	30.3	N	650	17.3	409.5	18.6	26.8	Y
NSA-I 2 / c = 350Nms/rad						**NSA-I 2 / c = 1600Nms/rad**					
260	10.2	249.3	5.2	44.9	N	510	16.1	518.7	6.9	38.6	Y
330	6.9	298.9	9.6	60.7	N	550	15.3	541.7	7.7	41.8	Y
400	5.7	338.9	14	74.6	N	590	14.4	571.2	8.7	46.1	N
NSA-I 3 / c = 350Nms/rad						**NSA-I 3 / c = 2100Nms/rad**					
180	10.8	237	6.4	39.7	N	420	19.5	556.7	8.6	33.2	Y
250	6.9	291.8	14	54.8	N	450	18.4	585.2	9.7	36.4	Y
320	5.9	324.7	20.9	63.4	N	490	17.3	620.4	11.3	40.5	N

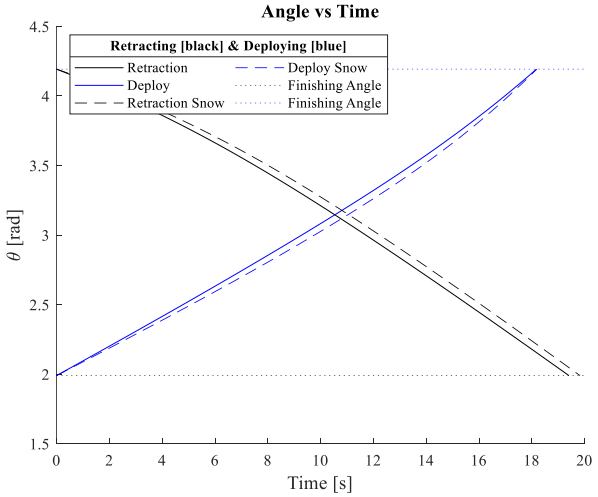

Figure 17: Cycle time for all motors

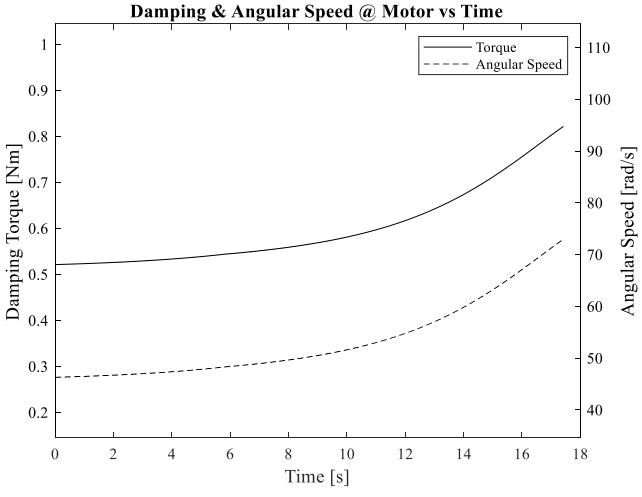

Figure 18: Damping torque and angular speed at the motor throughout motion

Table 6: Final characteristics of mechanism for selected motor, gear ratio and damping coefficient

Stall Torque [Nm]	No Load Speed [rpm]	Max Power [W]	Energy Used [J]	Deployment Time [s]	Retraction Time [s]
0.69	3650	39.4	558.1	18.2	19.4
Max Damping Torque [Nm]	Max Speed [rad/s]				
0.82	72.9				

D7. Damper Selection

The Kinetrol [12] catalogue was used to select the rotational damper based on the damping coefficient selected. Given that the layshaft would be turning up to a maximum rate of 697rpm, it was clear that continuous rotational dashpots (CRDs) had to be selected over vane dashpots, which were limited to turning between specified angles. This would be viable if attached to the output of the gearbox, however the torque at this stage would be far too high and in turn, result in a large 235mm x 235mm damper, weighing 12kg. This was unfeasible as in comparison, CRDs weighed in the hundreds of grams. The damper selected was model Q-CR (214g) as this had a maximum safe torque of 1.5Nm, sufficient for the maximum damping torque output of the final model. Using Fig. C in the Appendix, a viscosity of 12,500cSt was selected. As the damper was at the motor, the true damping coefficient is 2100 divided by the gear ratio, giving a final value of 4.98Nm/rad/s which is well within the effective range of 20Nm/rad/s stated on the catalogue. Final selection: Q-CRD-12500.

D8. Gearbox Design

D8.1. Gear & Module Selection

The gears chosen to be implemented in the gearbox were a combination of spur gears and a worm and wheel. Spur gears provide the advantages of high-power transmission alongside high efficiencies ranging between 96% to 99%. When considering Requirement 20 in the PDS to minimise cost, spur gears are especially suited due to the straight cut, involute profile making it simple to manufacture, hence cheaper than alternative gears. A worm and wheel were also considered as it allows for a very high velocity ratio, whilst also staying compact in size. Further advantages include a high loading capacity, operating without noise and minimal maintenance. Consequently, the primary disadvantage of worm drives would be their low efficiency which can reach values of 40% per stage since the surfaces are subject to high friction and axial stresses. Nevertheless, when paired with spur gears, which are the most efficient gear type available, the compromise of efficiency can be justified as the size of the gearbox would be greatly reduced for the velocity ratio achieved.

The velocity ratio to be achieved in the gearbox was determined in D6.3 and found to be between 420-450. A gear module needed to be selected, where the greater the value, the more load the gear can experience. From the gear module selection graph in Appendix Fig. B, the determined value for the module was roughly estimated to be between 0 and 1. Then, the maximum power values from Table 7 were used to find a corresponding angular velocity using (5).

$$P = -\left(\frac{T_{Stall}}{\omega_{no\ load}}\right)\omega^2 + T_{stall}\omega \qquad (5)$$

Table 7: Power values for gear ratio range

Gear Ratio	420	435	450
Max Power [W]	39	41	42

Where P is the power output, ω is the angular velocity, T_{Stall} is the stall torque and $\omega_{no\ load}$ is the no-load speed.

it was found that increasing the module consequently decreased the balanced bending stress as the critical tooth thickness increases by M number of times [13]. Therefore, maximising the module was ideal, which minimises the experienced wear over time. Thus, a module of 1 was taken forward for use in calculations.

D8.2. Gear Stages

A multi-stage gearbox system was chosen to be implemented as it allows for a high velocity ratio to be achieved whilst not compromising the size of the gearbox. Minimising the size can also result in a reduction in mass and possibly manufacturing costs. Consequently, selecting a multi-stage system can result in greater overall efficiency losses as more friction is generated within each stage. For a spur gear, the typical value for the maximum velocity ratio is 5. Any larger than this and the size of the driven gear would not be optimised to satisfy a compact gearbox. Alternatively, the velocity ratio of a worm and wheel can reach values up to 120 but can also lead to greater efficiency losses.

The selected number of stages was determined to be 3, with the initial stage consisting of the worm and wheel followed by 2 spur gear stages. When justifying the number of stages, an optimisation between reducing efficiency losses and minimising the size of the gearbox was considered. A rough calculation was made for a 3-stage gearbox to achieve a velocity ratio of 420. As an initial iteration, the velocity ratio per stage was selected as followed: 30:1 (worm), 4:1, 3.5:1.

According to KHK gears, the minimum number of teeth free of undercutting in a stock spur pinion for a standard pressure angle of 20° is 17 [14]. The repercussions of undercutting lead to a reduction in strength and also shortens the line of contact between meshing gears [15]. With a module of 1, the initial 3-stage configuration resulted in a total number of 192 teeth, including the pinion with a maximum gear diameter of 68mm. Consequently, when applying the same calculations to a single-stage system, the number of teeth calculated on the wheel was 7140 with a 7.14m diameter. Note that multi-stage gearboxes are typically designed with having the highest gear ratio at the input and a lower ratio at the output [16], explaining the decrease in gear ratios per stage.

The problem with this configuration is that during each revolution of the wheel, the same teeth in each of the meshing gears are always in contact with one another. Due to this, the wear is not evenly distributed amongst all the teeth and subsequently results in the shortening of the gear's life. To counteract this, the velocity ratio in each of the stages should have a hunting tooth gear combination. Thus, the improved gear ratios for each stage taking teeth hunting into account were: 30:1 (Worm), 70:17, and 58:17. Combined, this had a velocity ratio of 421.45, which is within the mentioned required range. The total number of teeth was calculated to be 192 including the 2 pinions in stages 2 and 3.

As the angular velocity of each stage decreases, the torque increases and therefore the tangential force experienced by the gears increase per stage. Varying the module in each stage was implemented to manage the increase in load. Applying (6) with the pinion angular velocity found in table 1 in stages 2 and 3, and calculating the corresponding power output, a module of 2 and 2.5 was determined respectively.

The number of starts in the worm was finalised to be 2. Applying the worm and wheel efficiency equation in (7), it was found that increasing the number of worms, also increases the efficiency.

$$\eta = \left(\frac{\tan(\varphi)}{\tan(\theta° + \varphi)}\right) \times 100 \qquad (6) \qquad\qquad \theta° = tan^{-1}(f) \qquad (7)$$

Where η is worm and wheel efficiency, φ is the lead angle and f is the coefficient of friction.

D8.3. Gear Characteristics & Manufacturer

Kohara Gear Industry (KHK) was chosen to be the manufacturer for gears as they provided an extensive selection and the required spur, worm and wheel gears based on the determined specifications. Prioritising cost and performance, the material chosen for spur gears was S45C steel. This is the most abundant material found in gears which directly reduces costs and displays a high strength-to-weight ratio, resistance to wear and the ability to enhance the physical properties through methods of temperature treatment [17]. KHK also includes a gear calculator which substantially simplifies loading calculations. Values for tangential and separating force which were determined using the calculator can be found in Table 8 and were calculated with a safety factor of 1.2, ensuring the loads experienced in the gears can be comfortably transmitted. The selected gears can be found in the bill of materials (Table 9). KHK didn't provide prices for the gears, therefore the cost of gears was sourced by an alternative manufacturer, HPC Gears, to provide a good estimate.

D8.4. Final Design

To minimise the size of the gearbox, overlapping lay shafts were used as seen in the Technical Drawing 4. A linear arrangement was immediately dismissed as the length of the gearbox would drastically increase. Due to the varying bore diameters between gears on the same lay-shaft, the lay-shaft was designed with a variable diameter. The lay shafts were also arranged so that they could be supported at both ends of the gearbox maximising the stability of the system.

Table 8: Gearing calculations and outputs

Gear Stage	**1**	**2**	**3**	**Gear Stage**	**1**	**2**	**3**
VR	30.0	4.118	3.412	Pinion speed, *RPM*	673.0	22.4	5.45
Combined VR	30.0	124	421.45	Wheel speed, *RPM*	22.4	5.45	1.60
Module	1	2	2.5	Pinion torque, *Nm*	0.560	16.80	69.2
Pinion teeth / *Worm Starts*	*2*	17	17	Wheel torque, *Nm*	16.80	69.2	236.0
Pinion PCD, *mm*	16.0	34.0	42.5	Pinion torque with losses, *Nm*	0.391	11.73	63.8
Wheel teeth	60	70	58	Wheel torque with losses, *Nm*	11.73	63.8	208.9
Wheel PCD, *mm*	60.1	140.0	145.0	Allowable tangential force, *kN*	0.536	2.12	3.31
Bore diameter pinion, *mm*	-	12	15	Tangential force, *kN*	0.3901	0.911	2.88
Bore diameter wheel, *mm*	10	18.0	20.0	Seperating force, *kN*	0.1420	0.3316	1.049
Efficiency, *%*	69.8	96.0	96.0	Resultant force, *kN*	0.4151	0.970	3.07
Combined efficiency, *%*	69.8	92.2	88.5				

Table 9: Bill of Materials (BoM)

Part	**Part number**	**Source**	**Quantity**	**Cost per unit (£)**	**Total cost (£)**
Alloy steel 4140 plate	AMS-S-6395	Metal Supermarkets	5	4.58	22.90
Alloy steel 4140 round bar	AMS-S-5626	Metal Supermarkets	5	1.34	6.70
Bushings	748-594	RS Components	14	2.10	29.40
Deep groove ball bearing	619-0171	RS Components	10	2.26	22.60
Motor	NSA-I 0 390 204 092	Bosch	1	42.32	42.32
Ultrasonic sensor	237-0783	RS Components	1	10.85	10.85
Hall effect sensor	479-6878	RS Components	1	10.43	10.43
Air flow sensor	619-1938	RS Components	1	93.40	93.40
Capacitive sensor	184-5598	RS Components	1	23.51	23.51
Worm shaft 1	KWG1-R2	KHK Gears	1	20.42	20.42
Wheel 1	CG1-60R1	KHK Gears	1	40.56	40.56
Pinion 1	SSG2-17	KHK Gears	1	14.25	14.25
Wheel 2	SSA2-70	KHK Gears	1	33.20	33.20
Pinion 2	SSG2.5-17	KHK Gears	1	21.70	21.70
Wheel 3	SS2.5-58	KHK Gears	1	69.61	69.61
Roof canvas material	A5B/DS	Haartz	1	215.30	215.30
					677.15

D9. Design Evaluation

Table 10: Product Solution Specification (PSS)

Requirement	**Target values**	**Result**	**Requirement**	**Target values**	**Result**
2	3000N	3032N	12, 13	80x80mm & 670x280mm	Targets met
3, 4, 5, 6	8mm, 20mph, 20mph respectively	Targets met - Mechatronics	14	25kg	23.5kg
7	No. of members and joints: 25	No. of members and joints: 20	15	300mm	253.93mm from Linkage
8	600mm	571mm	16, 17	Non-oxidising & recyclable	Targets met
9	Weatherproof casing	Target met	19	100%	Target met
10	Cycle time evenly split between motion phases	Target met	20	£500.00	£677.15
11	15s	Deploy: 18.2s Retract: 19.4s	21	Follow curves of base model 595	Target met

Evaluation of this project considers the overall design achieved, as well as critical review of the requirements initially set out. These outputs are analysed in Table 10, showing that the large majority of all targets were either exceeded or in the worst case, below the limit. The concept generation stage followed a rigorous process of sketching, Lego building, Linkage modelling and MATLAB modelling. Many design concepts and iterations were tested, with the belief that the chosen design has few weaknesses. These arise from project assumptions and estimates, and areas where activities were out of the scope of the brief, not allowing development and freedom of all aspects of the system. Further work would include building a prototype to establish a definite functional design. Further extensions for mechanism design were lucrative in providing representative outputs such as material selection to gain a realistic mass and FEA stress analysis to refine the geometry and attain maximum stress capacity, key to satisfying safety priorities set at the start. With regards to technical analysis and gear ratio/motor selection, an improvement would be to optimise the selection process and aim to cover all combinations as the manual process potentially overlooked better variables for the final design.

Overall, the design was not without flaws, but successful as a proof of concept design.

References

[1] Mini.co.uk. 2022. [online] Available at: <https://www.mini.co.uk/content/dam/MINI/marketUK/mini_co_uk/en_GB/brochures/MINI_F57_Convertible_Price_List_November_2018.pdf.asset.1539194089269.pdf> [Accessed 21 February 2022].

[2] 2022. How much weight can the convertible's roof hold?. [online] Available at: <https://www.bimmerfest.com/threads/how-much-weight-can-the-convertibles-roof-hold.506169/> [Accessed 13 March 2022].

[3] Snider, C., 2022. Engineering Practice Summative Project 2022.

[4] Car Throttle. 2022. How Convertibles Are Strengthened, And Why It's Beginning To Change. [online] Available at: <https://www.carthrottle.com/post/how-convertibles-are-strengthened-and-why-its-beginning-to-change/> [Accessed 22 February 2022].

[5] Iopscience.iop.org. 2022. ShieldSquare Captcha. [online] Available at: <https://iopscience.iop.org/article/10.1088/1757-899X/307/1/012040/pdf> [Accessed 5 May 2022].

[6] R. Ravivarman, "Effect of Module on Wear Reduction in High Contact Ratio Spur Gears Drive Through Optimized Fillet Stress," in Recent Advances in Theoretical, Applied, Computational and Experimental Mechanics, Singapore, Springer, 2020, pp. 239-250.

[7] EduPack, G., 2021. s.l.:Ansys Inc.

[8] process, p., process, c., reaction, c., group, v., location, m. and reaction, m., 2022. US7275783B2 - Convertible roof system with dampening device - Google Patents. [online] Patents.google.com. Available at: <https://patents.google.com/patent/US7275783> [Accessed 16 April 2022].

[9] Raymond, A., 2022. Dampers: SPD n-Struts® - Motion & Speed Control Dampers | Associated Spring Raymond. [online] Assocspring.co.uk. Available at: <https://www.assocspring.co.uk/dampers.html> [Accessed 12 April 2022].

[10] My.rs-online.com. 2022. Rotary Dampers | Adjustable Rotary Dampers | RS Components. [online] Available at: <https://my.rs-online.com/web/c/engineering-materials-industrial-hardware/anti-vibration-levelling-components/rotary-dampers/> [Accessed 1 May 2022].

[11] Bosch-ibusiness.com. 2022. [online] Available at: <https://www.bosch-ibusiness.com/media/images/products/dc_motors/xx_pdfs_2/pac_i-buisness_e-motors_21_22_cat_en_cd2016_82263.pdf> [Accessed 12 March 2022].

[12] Kinetrol.com. 2022. [online] Available at: <https://www.kinetrol.com/pdf/cat/Rotary_Damper_2013_LR.pdf> [Accessed 1 May 2022].

[13] Kohara Gear Industry Co.,Ltd., "Involute Gear Profile," 2021. [Online]. Available: https://khkgears.net/new/gear_knowledge/gear_technical_reference/involute_gear_profile.html#:~:text=The%20condition%20for%20no%20undercutting%20in%20a%20standard,strength%20and%20contact%20ratio%20pose%20any%20ill%20effect.. [Accessed 2 May 2022].

[14] Tec-Science, "Undercut of Gears," 2018. [Online]. Available: https://www.tec-science.com/mechanical-power-transmission/involute-gear/undercut/. [Accessed 2 May 2022].

[15] D. Collins, "What are multi-stage gearboxes and when are they used?," 2021. [Online]. Available: https://www.motioncontroltips.com/what-are-multi-stage-gearboxes-and-when-are-they-used/. [Accessed 2 May 2022].

[16] RoyMech, "Spur Gears - Design Process," 2020. [Online]. Available: https://roymech.org/Useful_Tables/Drive/Gears.html#:~:text=The%20gear%20face%20width%20should,60%25%20of%20the%20pinion%20diameter. [Accessed 2 May 2022].

[17] Gear Motions, "Selection of Gear Material," 2017. [Online]. Available: https://gearmotions.com/selection-of-gear-material/#:~:text=In%20our%20experience%2C%20at%20a,and%20the%20cost%20of%20manufacturing. [Accessed 2 May 2022].

[18]

ME Mechanical, 2017. Gruebler's Equation. [Online]
Available at: https://mechanicalengineering.blog/grueblers-equation/#:~:text=Degrees%20of%20freedom%20for%20planar,be%20calculated%20through%20Gruebler's%20equation.&text=Most%20linkages%20used%20in%20machines,shown%20in%20figure%20(a).
[Accessed 5 May 2022].

Appendix

Stakeholder	Involvement in Evaluation	Interest in Evaluation	Influence on Evaluation	Position	Impact of Evaluation on Stakeholder	Graph	
						Power	Interest
Group 1 Engineering Team	High: Major involvement. Primary team for all engineering evaluation	High: Directly involved in assessing the feasability and viability of the product being designed and created.	High: Main enginering team. Success of project is directly impacted by perfomance of this team.	Main engineering team will develop all aspects of the solution from the initial requirements. Will make main decisions on most aspects of the project and provide portfolio of documentation for evaluation for Fiat and marketable specifications for customers.	Evaluation will be used as performance marker which will have effect on personal development of team members, with a positive evaluation offering potential future opportunities.	8	9
FCA (Fiat Chrysler Automobiles)	High: Major resources provided to engineering subteam for R&D.	High: Potential for major return on invesment and alignment with company direction.	High: Main contributer of resources and alotted time to engineering team. Potential for project cancellation dependent on team performance and level of design.	Primary promotors and management of the project and will be providing both support and evaluation throughout all stages of project lifecycle. Will make final decision on project.	Results of final documentation and evluation of all stakeholders stance on the project will decide whether mass production and market placement commences. May offer future use of design adaptation in subsequent iterations of vehicles.	10	8
Manufacturers (Production Line)	Med: Will have to be involved in determining mass manufacturing methodology for production line implementation.	Med: Potential input and advice to tailor manufacturing methods towards current available facilities.	Low: It is assumed that manufacturing line should not be a bottleneck and given a successful evaluation, any proposed manufacturing methods should be integrated into production line.	Will provide specification limits for implementing solution design, could potentially limit concepts. Beyond this, should implement required machinery dependent on project success.	Will have an effect on whether production line is overhauled at all, on a small scale or on a large scale - dependant on success of project evaluation.	5	4
Suppliers (Components)	High: Major input from suppliers for available components and technology.	Med: Successful evaluation could influence future supply, availability and profit for suppliers - allowing for decreased purchase costs.	Med: Easy availability of certain components or wholesale deals could drive final solution design. Small lead times also drive faster development.	Will be providing physical hardware for product and full implementation. Influence comes from availability of components required and lead times which could influence design.	Successful evaluation results in increased business for supplier as the need to develop on a mass scale will be requested.	6	3
Investors	Low: Minor input at design stage however feedback taken on.	High: Offering personal capital and potential for high return on invesment following a successful evaluation.	High: Potential risk of capital loss could cause detrimental effects to project, possible cancellation.	Will be eager for communication and updates, keeping the engineering team on their toes as risk of pulling invesment should be expected at any failures.	Positive evaluation could see more investors and thus higher capital, allowing for future opportunities within company and higher standard of quality due to increased budgets on projects.	8	7
Customers	Low: Little to no input throughout engineering cycle - only exposed to final product at market.	High: Directly selling to customers thus final design will have to be satisfactory. Low: Will only need to communicated to once or twice before offical release, no need for consistent updates.	Med: As the primary intended customer, no sale could mean large losses.	Will be the primary customers to the final design however will not have too much influence on the project cycle, as design should meet the requirements of the majority, bar a niche subset who may not purchase final product.	In light of a negative evaluation, customers will not be aware of detailed specifics of the hypothetical design, and will have to 'deal' with current inefficient designs. Positive evaluation of course means increased satisfaction amongst those purchasing these vehicles and higher revenue for the company.	2	2

Figure A: Stakeholder matrix

Table A : Pairwise comparison weightings matrix

			=Much More Important	***=More*** Important	The ***=Same***	***=Less*** Important	***=MuchLess*** Important			
			9	3	1	0.333	0.111			
Criteria		Complexity	Max height	Mass	Torque	Safety	Cost	Stowed away size		
	X	1	2	3	4	5	6	7	Total	%
Complexity	1	X	0.33	1.00	3.00	0.11	9.00	3.00	16.44	13
Max height	2	3.00	X	3.00	9.00	0.11	0.33	9.00	24.45	19
Mass	3	1.00	0.33	X	1.00	0.11	0.11	1.00	3.56	3
Torque	4	0.33	0.11	1.00	X	0.11	0.11	1.00	2.67	2
Safety	5	9.01	9.01	9.01	9.01	X	1.00	9.00	46.04	36
Cost	6	0.11	3.00	9.01	9.01	1.00	X	9.00	31.13	25
Stowed away size	7	0.33	0.11	1.00	1.00	0.11	0.11	X	2.67	2
		13.79	12.90	24.02	32.02	1.56	10.67	32.00	126.95	100
		10.9	10.2	18.9	25.2	1.2	8.4	25.2	100	126.95

Table B: Weighted matrix for material selection

		Cast Iron, Ductile		Low Alloy Steel		Medium Carbon Steel		High Carbon Steel		Cast Al-Alloy		Age Hardening wrought Al-Alloys		Non-Age Hardening wrought Al-Alloys	
Criteria	**Weight**	**Value**	**Score**	**Value**	**Score**	**Value**	**Score**	**Value**	**Score**	**Value**	**Score**	**Value**	**Score**	**Value**	**Score**
Density (kg/m^3)	**3**	4	12	3	9	3	9	3	9	6	18	5	15	7	21
Price (GBP/kg)	**4**	7	28	4	16	6	24	5	20	2	8	1	4	3	12
Youngs Modulus (Gpa)	**1**	5	5	6	6	7	7	7	7	4	4	4	4	3	3
Yield Strength (GPa)	**4**	4	16	7	28	6	24	5	20	2	8	3	12	1	4
Tensile Strength (Mpa)	**2**	4	8	7	14	5	10	6	12	2	4	3	6	1	2
Compressive Strength (Mpa)	**2**	4	8	7	14	6	12	5	10	2	4	3	6	1	2
	Total		77		**87**		86		78		46		47		44

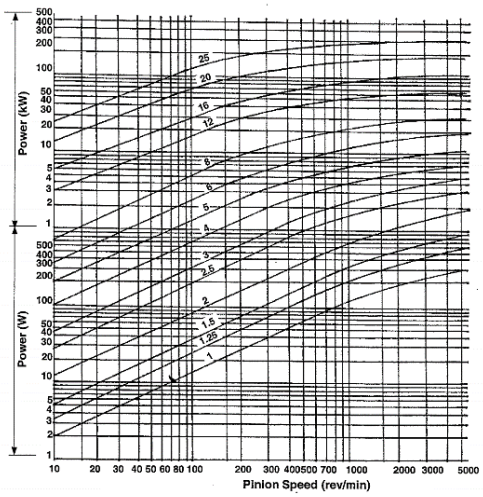

Figure B: Gear module selection charts

Type of Fit	Shaft tol.	Hole tolerance			
		H7	H8	H9	H11
Clearance	c11				▨
	d10			▨	
	e9			▨	
	f7		▨		
	g6	▨			
	h6	▨			
Transition	k6	▨			
	n6	▨			
Interference	p6	▨			
	s6	▨			

Table C: Tolerance table

Table D: Table to find upper/lower bound diameter

SELECTED ISO LIMITS AND FITS - HOLE BASIS

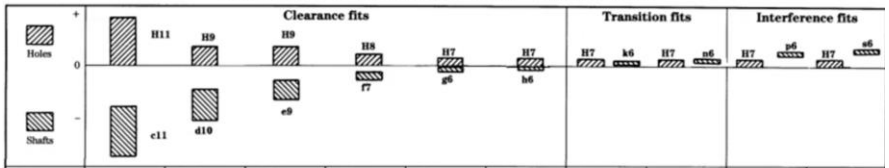

Nominal sizes		Tolerance		Tolerance		Tolerance		Tolerance		Tolerance		Tolerance		Tolerance		Tolerance		Tolerance		Tolerance	
Over	To	H11	c11	H9	d10	H9	e9	H8	f7	H7	g6	H7	h6	H7	k6	H7	n6	H7	p6	H7	s6
mm	mm	0.001mm	0.001mm	0.001mm	0.001mm	0.001mm	0.001mm	0.001mm	0.001mm	0.001mm	0.001mm	0.001mm	0.001mm	0.001mm	0.001mm	0.001mm	0.001mm	0.001mm	0.001mm	0.001mm	0.001mm
–	3	+60 0	-60 -120	+25 0	-20 -60	+25 0	-14 -39	+14 0	-6 -16	+10 0	-2 -8	+10 0	-6 0	+10 0	+6 +0	+10 0	+10 +4	+10 0	+12 +6	+10 0	+20 +14
3	6	+75 0	-70 -145	+30 0	-30 -78	+30 0	-20 -50	+18 0	-10 -22	+12 0	-4 -12	+12 0	-8 0	+12 0	+9 +1	+12 0	+16 +8	+12 0	+20 +12	+12 0	+27 +19
6	10	+90 0	-80 -170	+36 0	-40 -98	+36 0	-25 -61	+22 0	-13 -28	+15 0	-5 -14	+15 0	-9 0	+15 0	+10 +1	+15 0	+19 +10	+15 0	+24 +15	+15 0	+32 +23
10	18	+110 0	-95 -205	+43 0	-50 -120	+43 0	-32 -75	+27 0	-16 -34	+18 0	-6 -17	+18 0	-11 0	+18 0	+12 +1	+18 0	+23 +12	+18 0	+29 +18	+18 0	+39 +28
18	30	+130 0	-110 -240	+52 0	-65 -149	+52 0	-40 -92	+33 0	-20 -41	+21 0	-7 -20	+21 0	-13 0	+21 0	+15 +2	+21 0	+28 +15	+21 0	+35 +22	+21 0	+48 +35
30	40	+160 0	-120 -280	+62 0	-80 -180	+62 0	-50 -112	+39 0	-25 -50	+25 0	-9 -25	+25 0	-16 0	+25 0	+18 +2	+25 0	+33 +17	+25 0	+42 +26	+25 0	+59 +43
40	50	+160 0	-130 -290																		
50	65	+190 0	-140 -330	+74 0	-100 -220	+74 0	-60 -134	+46 0	-30 -60	+30 0	-10 -29	+30 0	-19 0	+30 0	+21 +2	+30 0	+39 +20	+30 0	+51 +32	+30 0	+72 +53
65	80	+190 0	-150 -340																	+30 0	+78 +59
80	100	+220 0	-170 -390	+87 0	-120 -260	+87 0	-72 -159	+54 0	-36 -71	+35 0	-12 -34	+35 0	-22 0	+35 0	+25 +3	+35 0	+45 +23	+35 0	+59 +37	+35 0	+93 +71
100	120	+220 0	-180 -400																	+35 0	+101 +79
120	140	+350 0	-200 -450	+100 0	-145 -305	+100 0	-84 -185	+63 0	-43 -83	+40 0	-14 -39	+40 0	-25 0	+40 0	+28 +3	+40 0	+52 +27	+40 0	+68 +43	+40 0	+117 +92
140	160	+250 0	-210 -460																	+40 0	+125 +100
160	180	+250 0	-230 -480																	+40 0	+133 +108
180	200	+290 0	-240 -530	+115 0	-170 -355	+115 0	-100 -215	+72 0	-50 -96	+46 0	-15 -44	+46 0	-29 0	+46 0	+33 +4	+46 0	+60 +31	+46 0	+79 +50	+46 0	+151 +122
200	225	+290 0	-260 -550																	+46 0	+159 +130
225	250	+290 0	-280 -570																	+46 0	+169 +140
250	280	+320 0	-300 -620	+130 0	-190 -400	+130 0	-110 -240	+81 0	-56 -108	+52 0	-17 -49	+52 0	-32 0	+52 0	+36 +4	+52 0	+66 +34	+52 0	+88 +56	+52 0	+190 +158
280	315	+320 0	-330 -650																	+52 0	+202 +170
315	355	+360 0	-360 -720	+140 0	-210 -440	+140 0	-125 -265	+89 0	-62 -119	+57 0	-18 -54	+57 0	-36 0	+57 0	+40 +4	+57 0	+73 +37	+57 0	+96 +62	+57 0	+226 +190
355	400	+360 0	-400 -760																	+57 0	+244 +208
400	450	+400 0	-440 -840	+155 0	-230 -480	+155 0	-135 -290	+97 0	-68 -131	+63 0	-20 -60	+63 0	-40 0	+63 0	+45 +5	+63 0	+80 +40	+63 0	+106 +68	+63 0	+272 +232
450	500	+400 0	-480 -880																	+63 0	+292 +252

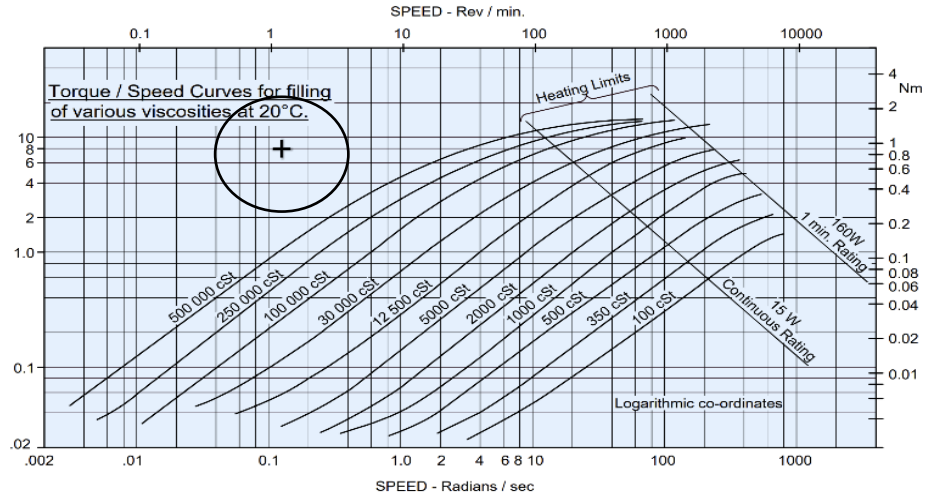

Figure C: Exert from Kinetrol catalogue – torque-speed curves for Q-CR dashpot fluid

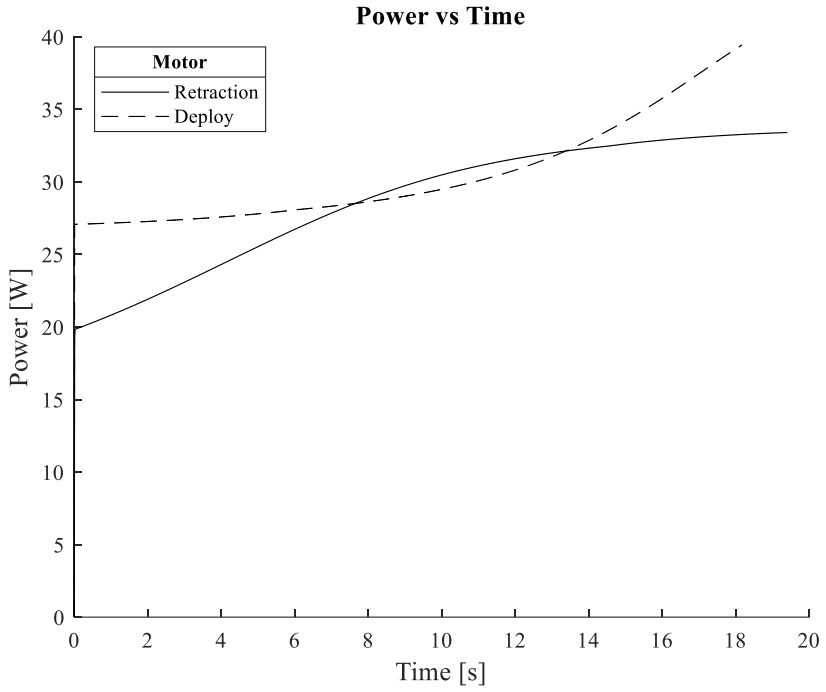

Figure D: Power vs Time for final design

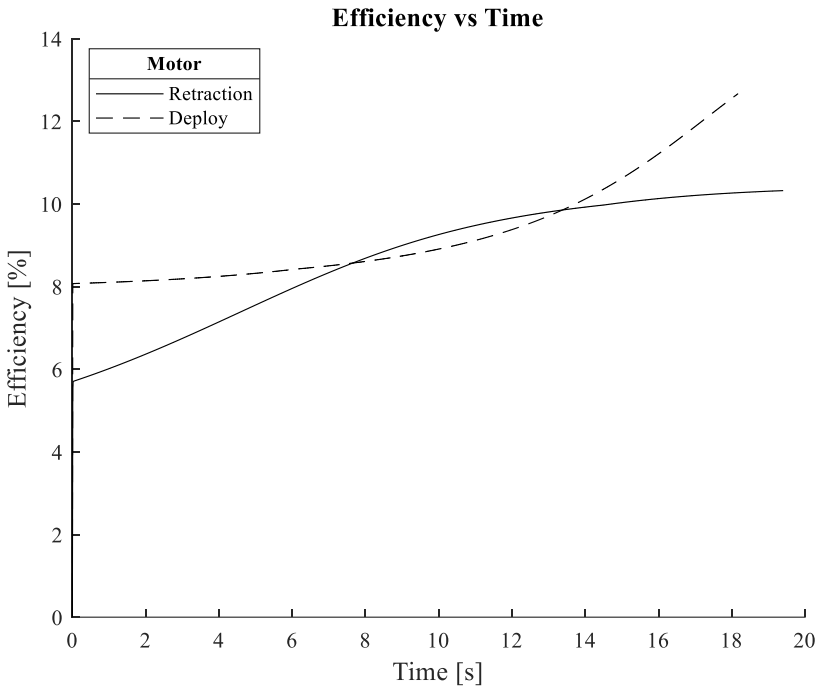

Figure E: Efficiency vs Time for final design